Isomerization and Hydrogenation of *cis*-2-Butene on Pd Model Catalyst

Björn Brandt,[†] Jan-Henrik Fischer,[†] Wiebke Ludwig,[†] Jörg Libuda,[‡] Francisco Zaera,[§] Swetlana Schauermann,*[,†] and Hans-Joachim Freund[†]

Fritz-Haber-Institut der Max-Planck-Gesellschaft, Faradayweg 4-6, 14195 Berlin, Germany, Lehrstuhl für Physikalische Chemie II, Friedrich-Alexander-Universität Erlangen-Nürnberg, Germany, and Department of Chemistry, University of California, Riverside, Riverside, California 92521

Received: January 9, 2008; Revised Manuscript Received: May 7, 2008

The adsorption and kinetics of conversion of *cis*-2-butene with deuterium on model supported Pd catalyst ($Pd/Fe_3O_4/Pt(111)$) were characterized by reflection−absorption infrared spectroscopy (RAIRS), temperature-programmed desorption (TPD), and isothermal molecular beam (MB) experiments. It was found that selectivity toward cis−trans isomerization and hydrogenation depends critically on the nature of the carbonaceous deposits, which are typically present during reaction on real catalysts. At low temperatures (190−210 K) both reaction pathways were found to proceed on the initially clean surface, but the catalytic activity was observed to quickly vanish, presumably because of the accumulation of hydrocarbon species on the surface. At temperatures above 250 K, on the other hand, a sustained catalytic activity toward cis−trans isomerization was observed over long periods of time. Interestingly, no catalytic activity could be sustained for the competing hydrogenation on the initially clean catalyst even at these temperatures. Only when highly dehydrogenated carbonaceous fragments were preadsorbed on the surface was it possible to induce a persistent catalytic activity for the hydrogenation (and also the isomerization) of the alkene on our supported palladium particles. Possible reasons of this unique vacuum catalytic behavior are discussed, including different spatial requirements for the competing reaction pathways and changes in the adsorption state of deuterium on and beneath the surface modified by the carbonaceous deposits.

1. Introduction

The promotion of alkene conversions, hydrogenation and isomerization in particular, is required for numerous chemical processes, including fine chemical and pharmaceutical synthesis, petrochemical hydrotreating, and food processing.[1,2] Alkene chemistry on metal surfaces has been extensively investigated in early years using conventional catalytic techniques[3,4,5] and also more recently by modern surface-science methodologies.[6,7,8] Although the surface-science approach has provided much insight into the mechanistic details of the key reaction steps on the catalyst surface, some important issues remain unresolved still. In particular, it is not clear what mechanisms govern selectivity in alkene conversions.

When promoted by transition-metal catalysts, alkene conversions such as hydrogenation, dehydrogenation, H-D exchange, and isomerization are generally accounted for by the so-called Horiuti-Polanyi mechanism,[9] which proceeds through a series of stepwise hydrogenation-dehydrogenation steps. In the particular case of the conversion of 2-butenes with hydrogen or deuterium, this mechanism involves the formation of a key surface butyl species via an initial half-hydrogenation of the adsorbed alkene; this species is generally believed to be a common reaction intermediate for the cis−trans isomerization, H-D exchange, and hydrogenation reaction pathways.[2,9–11] That butyl intermediate can then undergo a β-hydride elimination step to form an alkene, either the original molecule or one where cis−trans isomerization or double-bond migration has occurred (and a hydrogen has been replaced by a deuterium atom if deuterium is used as coreactant). Alternatively, the butyl moiety can follow a reductive elimination step with a second coadsorbed hydrogen or deuterium atom to form butane. Dehydrogenation of the adsorbed alkene to other surface species such alkylidynes is also possible.[12,13] Figure 1a provides a general scheme summarizing the possible conversions of *cis*-2-butene with deuterium.

In most of the studies on reaction selectivities published to date for alkene conversions under UHV conditions, H-D exchange has been found to dominate over the competing hydrogenation reaction. Thus, extensive H-D exchange has been observed for ethene on Ni(100)[14] and Rh(111),[15] for C_2-C_4 alkenes on Pd (100),[16] for C_6 alkenes on Pd(111),[17] and for ethene,[18–20] propene,[21] different C_4 (1-butene and *cis*- and *trans*-2-butenes),[15,22–25] C_5 alkenes,[26] and cyclic compounds[26,27] on Pt(111). In contrast, often only limited if any hydrogenation has been observed in those systems under the same UHV conditions. Several explanations have been provided for this. Guo and Madix[16] ascribed the absence of hydrogenation of the various alkenes they studied on Pd(100) to the strong hydrogen adsorption on that surface. Similarly, the weakening of metal−hydrogen bonds in the presence of coadsorbates was invoked to explain the promotion of alkene hydrogenation on both a Ni-precovered Pt(111) surface[28–30] and on a Fe(100) surface predosed with CO.[31,32] Zaera has suggested that the first half-hydrogenation to alkyl species may be the rate-limiting step in alkene hydrogenation, and that the β-hydride elimination then competes favorably against the reductive elimination step with coadsorbed hydrogen that leads to alkane production.[33,34]

More recently, the thermal chemistry of alkenes has been studied in our group on more realistic model catalysts consisting

* Corresponding author. E-mail: schauermann@fhi-berlin.mpg.de.
† Fritz-Haber-Institut der Max-Planck-Gesellschaft.
‡ Friedrich-Alexander-Universität.
§ University of California, Riverside.

10.1021/jp800205j CCC: $40.75
Published on Web 07/09/2008

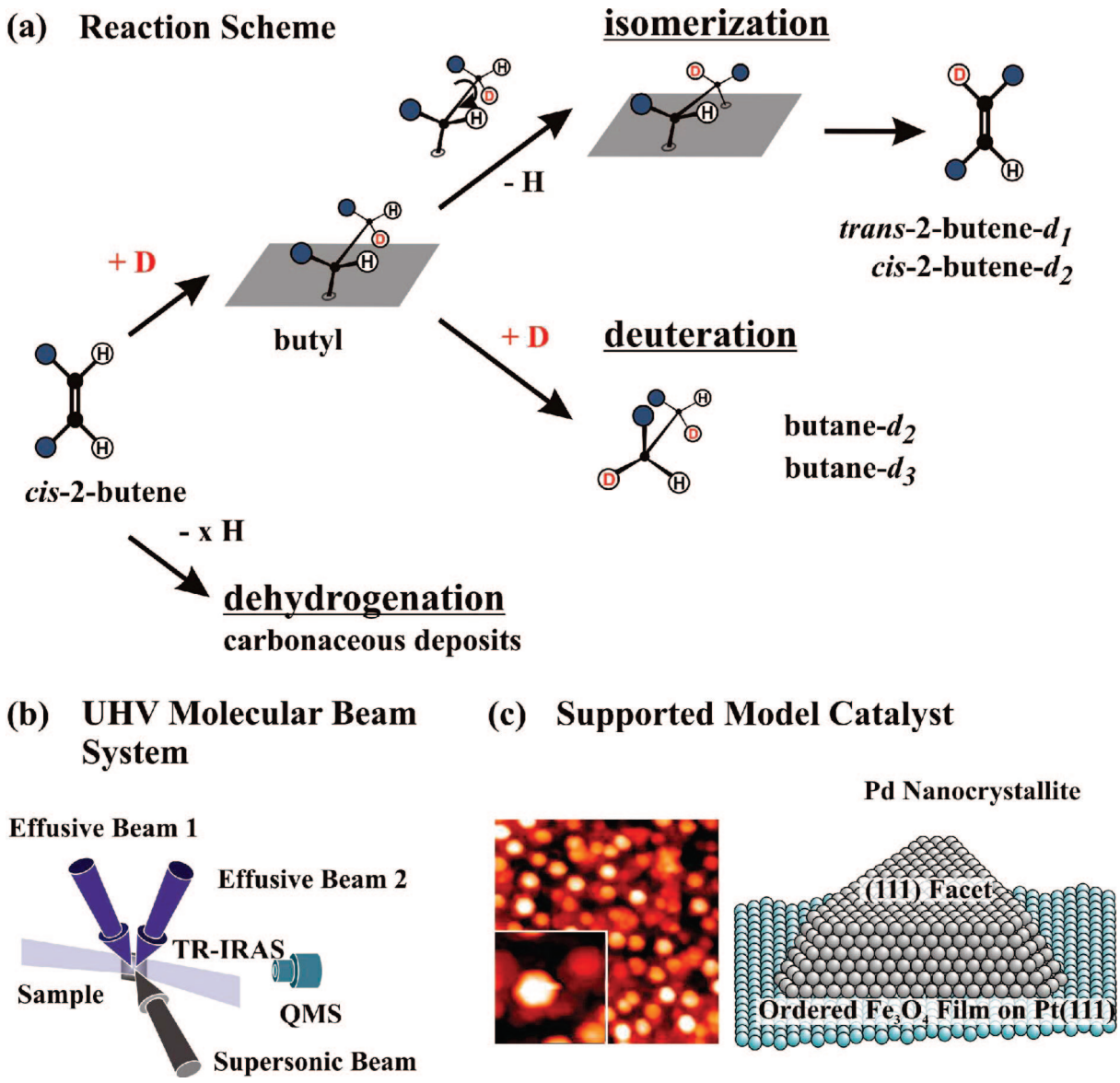

Figure 1. (a) Schematic representation of the three competing reaction pathways for *cis*-2-butene on Pd surfaces being considered in this study, namely: (1) cis−trans isomerization, which is accompanied by H-D exchange in the presence of coadsorbed deuterium, and which produces *trans*-2-butene-d_1 and *cis*-2-butene-d_2 as a mono- and doubly H-D exchanged/isomerized products, correspondingly, (ii) hydrogenation, which leads to the formation of butane (butane-d_2 and butane-d_3, the latter as a product of consecutive H-D exchange and deuteration steps), and (iii) dehydrogenation, which results in the formation of hydrocarbon fragments on the surface. (b) Schematic representation of the experimental setup for the molecular beam experiments. (c) Scanning tunneling microscopy (STM) image (100 nm × 100 nm, inset: 20 nm × 20 nm) of the Pd/Fe_3O_4/Pt(111) supported model catalyst used in the experiments described here, together with a schematic representation of the structure of the Pd nanoparticles in that catalyst.

of Pd nanoparticles supported on Al_2O_3/NiAl(110) oxide films.[35–39] In particular, it has been shown that, at least for ethene and *trans*-2-pentene, H-D exchange occurs on both Pd(111) single crystal and supported Pd particles, but hydrogenation proceeds only on the nanoparticles. Our experimental results strongly suggest that the formation of weakly bound subsurface hydrogen species, the accessibility of which is enhanced on nanoscale particles, is the key factor for the hydrogenation reaction to occur.

An additional complication to the understanding of hydrogenation and isomerization processes with alkenes arises from the fact that under catalytic conditions those are accompanied by an early decomposition of some of the reactants and the concurrent deposition of partly dehydrogenated carbonaceous species on the surface.[40–42] It has been determined in previous studies that, indeed, alkene conversions do not take place on clean metal surfaces but rather on metals covered by those strongly bound carbonaceous deposits.[43–47] Several stable surface intermediates originating from alkene thermal transformations have also been identified spectroscopically on various single crystal surfaces. The most extensive molecule studied to date in this respect is ethylene, from which ethylidene on platinum,[48–50] ethylidyne on palladium,[51,52] platinum,[53–58] rhodium,[59,60] ruthenium[61] and iridium,[62] vinyl on nickel,[63] palladium,[64] and platinum,[65,66] vinylidene on palladium,[67,68] and ethynyl on nickel,[69–71] platinum,[72] palladium[73] and rhodium[60] have been identified. Larger alkylidyne[24,74–79] and allylic[79–84] species have also been isolated when starting from heavier hydrocarbons. Those strongly adsorbed carbonaceous species, the alkylidynes in particular, are often considered mere spectators in catalytic reactions, but their exact role in the catalytic mechanism is still not known.

In this contribution, results are presented from our study of the kinetics of *cis*-2-butene conversion with deuterium over a model catalyst consisting of palladium nanoparticles supported on a Fe_3O_4 thin film. Particular emphasis is placed here on the understanding of the role of the carbonaceous deposits in defining the selectivity of the catalyst toward different reaction pathways such as hydrogenation and cis−trans isomerization/H-D exchange. Our ability to prepare well-defined supported model catalysts allowed us to design surfaces with a reduced level of complexity so they can be probed by surface-science techniques but which still mimic specific features of real catalysts.[85–89] The Fe_3O_4 thin oxide film was chosen as the support here to ensure high stability under reaction conditions.[90] A combination of molecular beam methods and infrared reflection−absorption spectroscopy[91] has been applied to obtain detailed isothermal surface kinetic data and to correlate those with vibrational spectroscopy evidence for the formation of different reaction intermediates on both clean Pd particles and surfaces precovered with specific types of carbonaceous deposits. The nature of those carbonaceous species is shown to critically control the activity and selectivity of the *cis*-2-butene conversion with deuterium. Particularly, both hydrogenation and isomerization reaction pathways are shown to proceed on the initially clean metal particles even at low temperatures (190−210 K). However, their catalytic activity quickly vanishes under those circumstances because of the accumulation of surface hydrocarbon species. At temperatures above 250 K, a sustained catalytic activity toward cis−trans isomerization/H-D exchange is observed, but no steady-state hydrogenation rate could be detected. Most interestingly, it is shown that under the same reaction conditions a surface precovered with carbon exhibits a persistent catalytic activity toward both cis−trans isomerization and hydrogenation. This implies that the carbonaceous species resulting from the early decomposition of the reactants are not merely spectators in alkene conversions, but rather modify the adsorption properties of the surface and critically control selectivity. Possible reasons of this unique catalytic behavior, including different spatial requirements of the competing reaction pathways and changes in the adsorption state of deuterium on the surface modified by the carbonaceous deposits, are discussed. In addition, it is also reported here that alkene conversion on our model catalytic surfaces can be sustained over long times under our vacuum conditions, something that, to the best of our knowledge, has not been achieved before.[92,93]

2. Experimental Section

All molecular beam (MB), temperature programmed desorption (TPD), and reflection−absorption infrared spectroscopy (RAIRS) experiments were performed at the Fritz-Haber-Institut (Berlin) in a UHV apparatus described in detail previously.[91] A schematic representation of the setup is shown in Figure 1b. Briefly, this system offers the experimental possibility of crossing up to three molecular beams on the sample surface. An effusive, doubly differentially pumped multichannel array source was used to supply the D_2. This beam was modulated using remote-controlled shutters and valves. Beam fluxes for D_2 of 3.2×10^{15} molecules cm^{-2} s^{-1} were used in these experiments. The source was operated at room temperature. The beam diameter was chosen such that it exceeded the sample diameter. A supersonic beam, generated by a triply differentially pumped source and modulated by a solenoid valve and a remote-controlled shutter, was used to dose the *cis*-2-butene (Aldrich, >99%) at a flux of 5.6×10^{12} molecules cm^{-2} s^{-1} (typical backing pressure: 1.15 bar). The diameter of this beam was chosen to be smaller than the sample for the experiments discussed here. Modulation of the beams, in particular that of the butene, was performed to differentiate between the products desorbing from the sample because of chemical reactions and any other interfering signals such as a slowly growing background observed over the course of the experiments. It should also be noted that the steady-state experiments reported below were carried out at temperatures well above those required for the desorption of the olefins. Therefore, they reflect the kinetics of the chemical reactions on the surface, not that of the desorption of the hydrocarbons. An automated quadrupole mass spectrometer (QMS) system (ABB Extrel) was employed for the continuous and simultaneous monitoring of the partial pressures of the reactants (2-butene, followed by the signal of the $C_3H_5^+$ fragment at 41 amu because of experimental reasons) and products (2-butene-d_1, $C_3H_4D^+$ fragment at 42 a.m.u.; 2-butene-d_2, $C_3H_3D_2^+$ fragment at 43 a.m.u.; butane-d_2, $C_3H_5D_2^+$ fragment at 45 a.m.u., and butane-d_3, $C_3H_4D_3^+$ fragment at 46 a.m.u.). All QMS data have been corrected to account for the natural abundance of C_{13} in all the molecules followed in our experiments. TPD experiments were carried out in the same vacuum system and by using the same QMS instrumentation. Linear heating ramps for the sample were set to a value of 3.5 K s^{-1}. RAIRS data were acquired by using a vacuum Fourier-Transform Infrared (FT-IR) spectrometer (Bruker IFS 66v/S) with a spectral resolution of 2 cm^{-1}, using a mid-infrared (MIR) polarizer to select the p-component of the IR light.

The Pd/Fe_3O_4 model catalyst was prepared as follows: the thin (∼100 Å) Fe_3O_4 film was grown on a Pt(111) single crystal surface by repeated cycles of Fe (>99,99%, Goodfellow) physical vapor deposition and subsequent oxidation (see refs 90 and94–96 for details). The cleanliness and quality of the oxide film was checked by RAIRS of adsorbed CO and by LEED. Pd particles (>99.9%, Goodfellow) were grown by physical vapor deposition using a commercial evaporator (Focus, EFM 3, flux calibrated by a quartz microbalance) while keeping the sample temperature fixed at 115 K. During Pd evaporation, the sample was biased to +800 V in order to avoid the creation of defects by metal ions. The final Pd coverage used in these experiments was 2.7×10^{15} atoms cm^{-2}. The resulting surfaces were then annealed to 600 K, and stabilized via a few cycles of oxygen (8×10^{-7} mbar for 1000 s) and CO (8×10^{-7} mbar for 3000 s) exposures at 500 K before use.[90] An STM image of the model surface resulting from this preparation is shown in Figure 1c. That surface displays Pd particles with an average diameter of 7 nm, containing approximately 3000 atoms each, and cover the support uniformly with an island density of about 8.3×10^{11} islands cm^{-2}.[90] It should be noted that the size of the Pd particles appears substantially larger in these STM images because of the convolution of the signal with that of the tip used as the probe. An accurate estimation of Pd dispersion shows that only about 20% of the support surface area is covered with nanoparticles.[90] The majority of the particles are well-shaped crystallites grown in the (111) orientation and are predominantly terminated by (111) facets (∼80%), but a small fraction of (100) facets (∼20%) is also exposed.

3. Results and Discussion

3.1. *cis*-2-Butene Adsorption and Conversion with Deuterium on the Fe_3O_4 Film. As a first step, the adsorption properties and the reactivity of the bare Fe_3O_4 support for *cis*-2-butene conversion with deuterium was considered. For that, pulsed molecular beam experiments were performed under

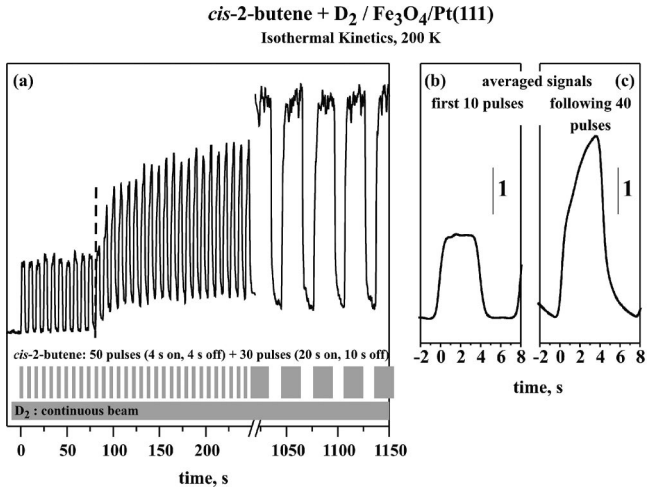

Figure 2. (a) Pulse sequence and time evolution of the *cis*-2-butene mass spectrometry signal during a typical isothermal pulsed molecular beam (MB) experiment for the conversion of *cis*-2-butene with D_2 at 200 K on our Fe_3O_4 model support. The sample was first exposed to a continuous D_2 beam (flux 3.2×10^{15} molecules cm^{-2} s^{-1}), after which a second modulated *cis*-2-butene beam (flux 5.6×10^{12} molecules cm^{-2} s^{-1}) was introduced. Typical MB sequences included 50 short pulses (4 s on, 4 s off time) followed by 30 longer pulses (20 s on, 10 s off time). (b) Averaged *cis*-2-butene signal for the first 10 pulses, indicating strong irreversible adsorption. (c) Averaged *cis*-2-butene signal for the following 40 pulses showing a weak reversible adsorption behavior.

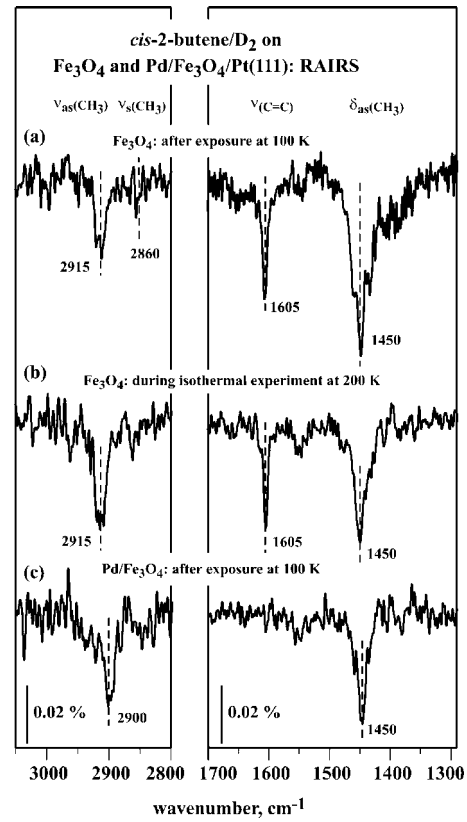

Figure 3. RAIR spectra obtained (a) on the Fe_3O_4 film after sequentially dosing 280 L of deuterium and 0.85 L of *cis*-2-butene at 100 K, (b) on the Fe_3O_4 film during the isothermal MB beam experiment at 200 K shown in Figure 2, and (c) on the supported Pd/Fe_3O_4 catalyst after sequentially dosing 280 L of deuterium and 0.8 L of *cis*-2-butene at 100 K.

isothermal conditions at 200 K. Figure 2a displays a typical pulse sequence and the time evolution of the partial pressure of the reactant in the vacuum chamber during the run. In this experiment, the sample was continuously exposed to a D_2 beam during the complete experiment. Subsequently, the *cis*-2-butene was switched on and off, starting after 90 s from the beginning of the D_2 dosing. A typical MB sequence included 50 short butene pulses (4 s on, 4 s off time) followed by 30 longer pulses (20 s on, 10 s off time). The time evolution of the reactant signal displayed in Figure 2a clearly shows two distinct adsorption modes for *cis*-2-butene on the bare Fe_3O_4 film. First, during the first 10 short pulses, the butene sticks effectively to the oxide surface, leaving behind only a small fraction of the original beam intensity in the gas phase. After that, the gas-phase signal during exposure to butene increases substantially, indicating a lower sticking probability on the Fe_3O_4 support. Additional information on the butene adsorption behavior in these two adsorption modes can be extracted from the analysis of the pulse shapes, shown in detail in Figure 2b. These were calculated by averaging the *cis*-2-butene traces for the first 10 pulses and the following 40 pulses for the "strong" and "weak" adsorption modes, respectively. The first adsorption regime is characterized by a square pulse shape and a high sticking probability, of about 0.65 as calculated by the ratio of the partial pressure reached here to the partial pressure at the end of the run, indicating strong and irreversible adsorption of butene species on the surface. This strongly adsorbed state saturates after approximately 2×10^{14} molecules/cm^{-2} are deposited on the surface. In contrast, the pulse shape of the second adsorption mode deviates clearly from such a square shape. It displays an initial fast increase after switching on the butene beam and a slower growth of the signal upon continuing exposure. This behavior suggests that in this mode some butene adsorbs reversibly on the Fe_3O_4 surface, already covered by the more strongly bonded adsorbate species. It is worth noting that this behavior originates exclusively from butene adsorption on the Fe_3O_4 support and does not reflect a saturation process of the chamber walls (this possibility was ruled out by control experiments where the butene was dosed onto the gold flag instead of the sample). Another important observation here is the fact that no gas-phase reaction products were detected in these isothermal MB experiments, indicating that the Fe_3O_4 surface alone is inactive toward both hydrogenation and H-D exchange/isomerization of the alkene (data not shown). The lack of reactivity of the oxide film was corroborated by TPD experiments carried out on the clean and deuterium-precovered oxide support: only molecular desorption of the reactant was observed in those cases, at 335 K on the clean surface and between 240 and 290 K on the deuterium-preexposed oxide film (data not shown). This result is in good agreement with the previously reported lack of C−H bond activation in alkenes on the Fe_3O_4 surfaces.[97–99]

Molecular *cis*-2-butene adsorption was also confirmed directly by RAIRS data. The top two traces of Figure 3 show IR spectra recorded after dosing the alkene on a deuterium-predosed bare oxide surface at 100 K (Figure 3a) and during the isothermal MB experiment at 200 K discussed above (Figure 3b). Four absorption bands dominate both spectra: the asymmetric methyl deformation ($\delta_{as}(CH_3)$ at 1450 cm^{-1}), the C═C stretching (ν(C═C) at 1605 cm^{-1}), and the symmetric and asymmetric C−H stretching of the terminal methyl groups ($\nu_s(CH_3)$ and $\nu_{as}(CH_3)$ at 2860 and 2915 cm^{-1}, respectively).[100–103] The presence of the carbon−carbon double bond vibration at 1605 cm^{-1} in particular attests to the previous conclusion concerning the molecular nature of *cis*-2-butene adsorption on the oxide surface. In fact, adsorption of butene may be relatively weak, since the C═C double bond does not undergo the strong sp^3 rehybridization due to formation of a di-σ bonded complex

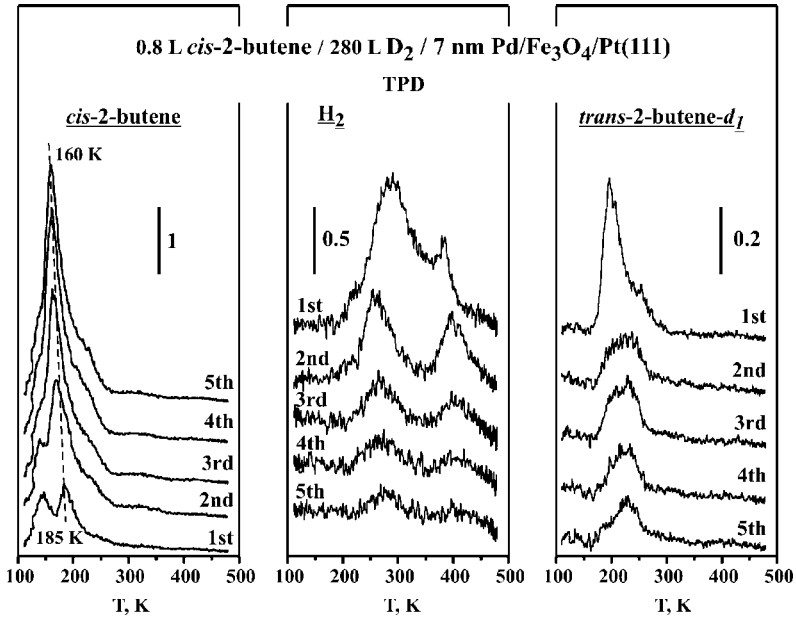

Figure 4. *cis*-2-Butene (left panel), hydrogen (center panel), and *trans*-2-butene-d_1 (right panel) temperature programmed desorption (TPD) traces obtained after sequential dosing of 280 L of D_2 and 0.8 L of *cis*-2-butene at 100 K on our Pd/Fe_3O_4 model catalyst. Data are reported for five consecutive experiments carried out by ramping the temperature to up to 500 K each time and dosing the reactants on the surface resulting from the previous experiment without any intermediate treatment. Particularly noteworthy here is the persistent signal obtained for *trans*-2-butene-d_1 production (right panel) after the repeated experiments, indicating sustained reactivity toward isomerization even after the build up of a carbonaceous layer on the surface.

typically seen for alkenes on metal surfaces.[10,13,23,104,105] On the other hand, the vibrational frequency of ν(C═C) shifts by about 55 cm^{-1} compared to its gas-phase value (1660 cm^{-1}), suggesting a relative strong interaction of the adsorbed alkene with the Fe_3O_4 surface more than what would be expected from simple physisorption. Additionally, based on the metal surface selection rule (MSSR) that applies to RAIRS with metals,[106,107] it may be inferred from the attenuation of the peaks for the symmetric CH_3 stretching (2870 cm^{-1}) and deformation (1375 cm^{-1}) as well as the in-plane C−H deformation (1403 cm^{-1}) modes that the adsorption geometry of the alkene is nearly flat on the oxide support.

3.2. Adsorption and Decomposition of *cis*-2-Butene on Pd Particles Supported on the Fe_3O_4 Film in the Presence of Coadsorbed Deuterium. Next, the adsorption and decomposition of butene in the presence of deuterium on the Pd particles was characterized by temperature-programmed desorption (TPD) experiments. Figure 4 displays TPD spectra obtained after sequentially dosing approximately 280 L of D_2 and 0.8 L of the alkene at 100 K. Those exposures were chosen to ensure near saturation of the surface with both atomic deuterium and molecular butene. Five TPD data sets were obtained sequentially by ramping the temperature up to approximately 500 K, cooling down to 100 K, and redosing the reactants without cleaning or any other treatment of the surface in between experiments in order to test the effect of the carbonaceous deposits that build up on the surface on its reactivity.

The H_2 TPD trace obtained from the first experiment (Figure 4, center panel, top trace) indicates a threshold for hydrocarbon decomposition at about 200 K and a stepwise dehydrogenation with peaks around 285 and 385 K. It should be kept in mind, however, that the first H_2 desorption peak at 200 K might be limited by associative hydrogen desorption, which means that hydrocarbon decomposition may begin even at lower temperatures. Much more limited decomposition is seen after the first TPD, but reproducible small peaks are observed in all subsequent traces with desorption maxima at about 275 and 400 K (Figure 4, center panel, four bottom traces). The inhibition of the dehydrogenation reactions after the initial TPD is accompanied by an increase in molecular desorption from a weakly bound state. This is manifested by the molecular TPD peaks at 145 and 185 K, evolving into a larger feature peaked at 160 K and a small shoulder around 230 K (Figure 4, left panel). Extensive isomerization and H-D exchange of the alkene on the surface is also observed: a substantial amount of monodeuterated *trans*-2-butene-d_1 is produced at 200 K and, to a lesser extent, at 255 K on the clean surface, and detectable C_4H_7D production is still observed after five TPDs, mostly at 230 K (Figure 4, right). It should be mentioned that doubly exchanged/doubly isomerized *cis*-2-butene-d_2 was also found to desorb around 200 and 250 K, in peaks that change little with the number of TPDs performed, and that deuteration to butane-d_2 was observed at 205 and 235 K on the clean surface (data not shown). The hydrogenation (deuteration) reaction is completely suppressed after the first TPD (data not shown). No other products from butene conversion with deuterium were observed.

The nature of the surface adsorbates originating from *cis*-2-butene exposure on the supported Pd clusters was investigated by RAIRS. Figure 3 shows a comparison of the RAIRS data obtained after *cis*-2-butene exposure on the pure Fe_3O_4 film (Figure 3a) versus on the Pd particles supported on this oxide surface (Figure 3c). Both surfaces were pretreated with 280 L of deuterium before exposure to the alkene, and the spectra were taken at 100 K. The IR spectra obtained on the supported metal particles show pronounced differences as compared to the pristine oxide film: whereas two of the main features, the asymmetric methyl deformation $\delta_{as}(CH_3)$ at 1450 cm^{-1} and asymmetric C−H stretching of the terminal methyl groups $\nu_{as}(CH_3)$ at 2900 cm^{-1}, remain nearly the same (the $\nu_{as}(CH_3)$ peak shifts slightly from the original 2915 cm^{-1} value), the third prominent vibration for the C═C stretching, ν(C═C), at 1605 cm^{-1}, vanishes completely in the spectra on Pd particles. This indicates a strong rehybridization of the double bond and the formation of a di-σ complex on the metal surface. It is worth

noting that even though, according to STM data,[90] about 80% of the Fe_3O_4 surface is still exposed in the system with the supported Pd particles, no support-related butene species were observed in the IR spectra. This fact suggests that either the adsorption properties of the support are strongly modified after Pd deposition and stabilization under oxidizing conditions, or that butene diffuses rapidly from the support to the metal particles, where it binds more strongly.

In light of these results it is concluded that decomposition of *cis*-2-butene on the supported Pd particles proceeds in a similar manner as on Pt and Pd single-crystal surfaces.[16,22,23,25,75,76,108–110] In particular, there is good agreement between the hydrogen TPD traces obtained here and those reported in the literature from single crystals in terms of both peak positions and relative intensities.[22,75] Additionally, the low-temperature RAIRS data obtained on the Pd particles in this study are consistent with the formation of a di-σ surface species in the submonolayer regime, in the same way as previously observed spectroscopically on Pt[23,75,103] and Ru.[110] Based on these data as well as on previous reports on similar systems[10,104,108] we may speculate that *cis*-2-butene adsorbs on the Pd particles via the formation of a di-σ bound species in the submonolayer coverage around 100 K, and dehydrogenates to a di-σ bonded 2-butyne species at room temperature and to highly dehydrogenated carbonaceous deposits (presumably C_4H_2) above 400 K.

3.3. H-D Exchange, Isomerization, and Hydrogenation of *cis*-2-Butene on Pd Particles Supported on the Fe_3O_4 Film. As mentioned above in reference to the TPD results in Figure 4c, the thermal activation of *cis*-2-butene coadsorbed with deuterium on our Pd model catalyst leads to extensive isomerization and H-D exchange of the alkene. In addition to the substantial production of monodeuterated *trans*-2-butene at 200 and 255 K on the clean surface and at 230 K after the first TPD, some doubly exchanged/doubly isomerized *cis*-2-butene is also made at approximately the same temperatures, and deuteration to butane-d_2 is observed at 205 and 235 K on the clean surface. These results are also, in general terms, in agreement with previous work on Pd(100)[16] and Pt(111)[22,25] single crystals. While no hydrogenation products have been detected for any of those alkenes on either surface, extensive H-D exchange (accompanied by cis−trans isomerization in the case of the 2-butenes) has been reported both for 1- and 2-butenes. Also, *cis*- and *trans*-2-butenes were shown to form only mono and doubly deuterium-substituted species on Pt(111), presumably because only the inner hydrogen atoms can be exchanged; this observation is in full agreement with our experiments on the supported Pd particles. However, there are also some important differences in the alkene conversion on the metal clusters versus the single crystals. For example, the majority of the H-D exchange/isomerization products in the first TPD run in this study desorbs at temperatures significantly lower than those reported for Pt(111) (200 vs 260 K). Also, even though the low-temperature H-D exchange channel seen in Figure 4 shuts off on the surface pretreated with hydrocarbons (that is, after the first TPD run), persistent H-D exchange is still observed at 230 K in all of the following TPD experiments. This shows that the surface is capable of maintaining its H-D exchange activity in the presence of large amounts of highly dehydrogenated carbonaceous deposits, something that is also not typical on single crystals.

The observation of persistent catalytic activity on the supported Pd particles suggests that free metal sites are still exposed on the surface precovered with highly dehydrogenated carbonaceous deposits. To verify this hypothesis, the availability of metal surface sites for reaction was evaluated by performing CO adsorption experiments. The RAIRS spectra obtained on the clean and C-precontaminated Pd particles are shown in Figure 5. The CO spectrum for the clean surface (bottom trace) is dominated by an intense and sharp peak centered around 1978 cm^{-1}, associated with Pd sites on the particle edges and corners and to a lesser extent with (100) facets.[111,112] The broad features between 1960 and 1800 cm^{-1} are attributed to CO adsorption on the regular (111) facets representing the majority of the surface sites.[111,112] It should be pointed out that the intensities of the IR signals are expected to be strongly modified by dipole-coupling effects[113] and, as a consequence, to not directly reflect the relative abundance of the corresponding sites. In the particular case of the Pd particles, the feature at high frequency corresponding to the low-coordinated sites (edges, corners, etc.) is likely to gain intensity at the expense of the absorption signal at lower frequency related to the regular (111) facets. In any case, the main effect of the deposition of carbonaceous species during the TPD runs reported here is the complete disappearance of the 1978 cm^{-1} peak; the spectral features in the low-frequency region remain nearly unchanged. Additionally, a new peak grows at 2095 cm^{-1} associated with on-top adsorption sites. These changes indicate preferential adsorption of carbonaceous deposits on the edges, corners, and (100) facets, and the fact that regular terraces remain considerably less contaminated. A similar behavior has previously been observed for carbon deposits generated by methanol decomposition.[114,115] Recent DFT calculations also support preferential adsorption of carbon at the edges of Pd clusters and suggest that part of the carbon atoms may be located in subsurface sites.[116]

Another interesting observation here is the ability of the initially clean supported particles to hydrogenate the double bond of the olefin, a reaction that is not seen on palladium single crystals. It should be noted that while alkenes tend to desorb

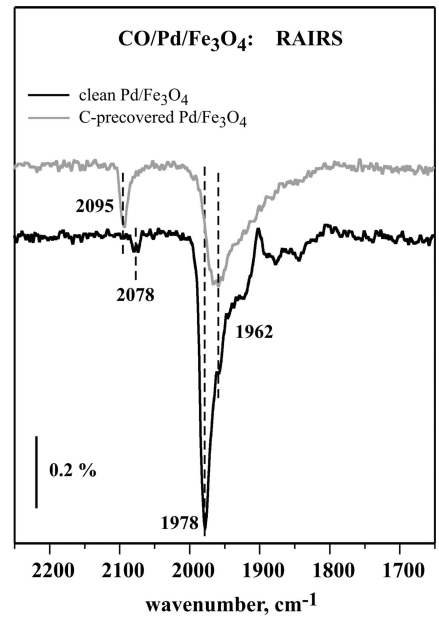

Figure 5. CO RAIRS titration spectra for $Pd/Fe_3O_4/Pt(111)$ surfaces clean (bottom) and after the first TPD experiment shown in Figure 4, which leads to the deposition of highly dehydrogenated carbonaceous species. The surface was saturated with CO at room temperature and cooled to 100 K before data acquisition. The data indicate that carbon deposition on the palladium particles leads mainly to blocking of both low-coordination defect (edges, corners) sites and bridge sites on (100) facets. The majority of the surface sites on the regular (111) terraces remain unaffected.

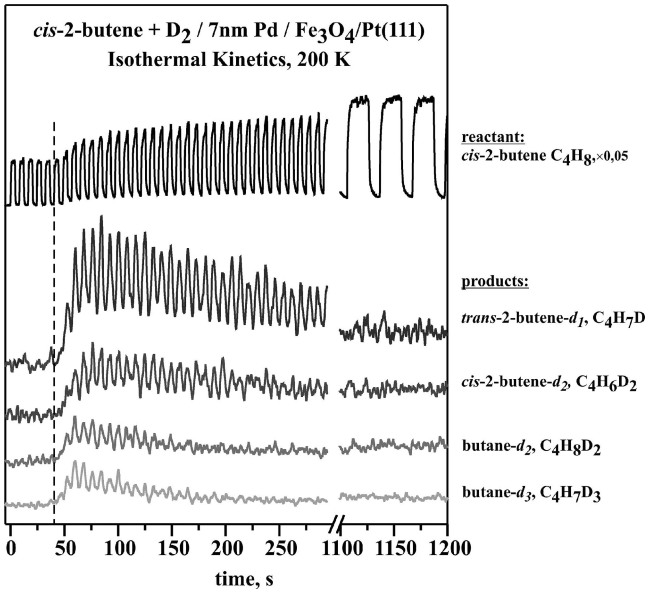

Figure 6. Results from an isothermal kinetic MB experiment carried out at 200 K on Pd/Fe_3O_4 by using the same pulse scheme described in Figure 2. Shown is the time evolution of both the reactant (*cis*-2-butene) and the products (*trans*-2-butene-d_1, *cis*-2-butene-d_2, butane-d_2, and butane-d_3). The reaction rates display a pronounced induction period followed by a transient regime of high activity toward both H-D exchange/isomerization and hydrogenation reaction pathways. However, after a few hundreds of seconds, all reaction rates return to zero.

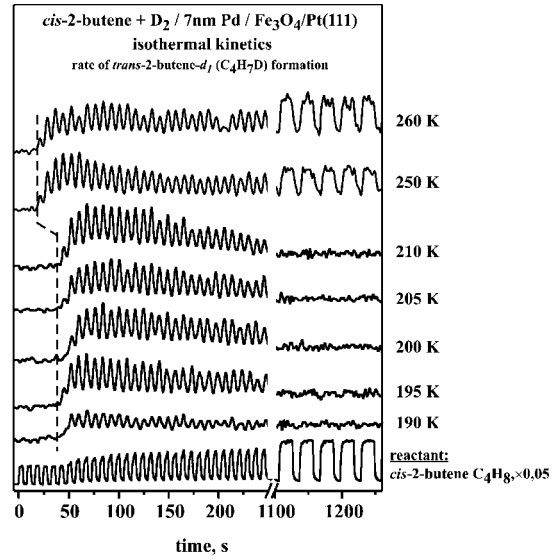

Figure 7. Results from MB experiments carried out on Pd/Fe_3O_4 at different temperatures in the range from 190 to 260 K, again using the MB pulse scheme described in Figure 2. Shown is the time evolution of the product of cis−trans isomerization (*trans*-2-butene-d_1) for each temperature, together with that of the reactant (*cis*-2-butene, bottom trace). Below 210 K the reaction rates are high at the beginning but return to zero after prolonged exposures. Above 250 K, on the other hand, there is a shorter induction period, and sustained catalytic activity toward isomerization is possible.

molecularly rather than hydrogenate on single crystals,[38,117] extensive conversion has been reported already for ethylene and *trans*-2-pentene hydrogenation on Pd particles dispersed on thin oxide films.[35,39] This difference has been ascribed to the ability of the dispersed particles to absorb highly reactive hydrogen atoms in a weakly bound subsurface state.[37]

The significant desorption of H-D exchange products in the TPD experiments described above after deposition of hydrocarbon fragments on the surface strongly suggests that it may be possible to sustain steady-state conversion on these surfaces. This hypothesis was indeed confirmed by the molecular beam experiments described next. Additionally, the differences in the catalytic behavior between the initially clean Pd particles and the particles precovered with hydrocarbon fragments indicate that not only activity but also selectivity depends strongly on the nature of the carbonaceous species present on the surface during the catalytic reaction.

3.4. cis-2-butene conversion with deuterium on Pd/Fe_3O_4: isothermal molecular beam experiments. In order to further investigate the activity and selectivity of the Pd/Fe_3O_4 model catalyst for *cis*-2-butene conversion with deuterium, and to explore the effect of the carbonaceous deposits, pulsed isothermal molecular beam experiments were performed by applying the same D_2 and *cis*-2-butene dosing scheme used for the studies on the bare Fe_3O_4 support (see Section 3.2). Figure 6 displays the reaction rates of both reaction pathways, H-D exchange/isomerization and hydrogenation, obtained at 200 K on the initially clean surface (lower 4 traces), together with the trace for the reactant uptake during the MB run (uppermost trace). In general, the *cis*-2-butene uptake here exhibits a similar behavior to that observed on the bare Fe_3O_4 support, with the two distinct adsorption modes identified above: (i) a strong irreversible adsorption at the beginning of the exposure, with a high sticking probability ($S = 0.65$) and a square pulse shape, and (ii) a subsequent weaker and reversible adsorption, with the surface concentration of the alkene increasing upon admission of the beam and decreasing after beam termination. However, initial saturation of the supported catalyst with the strongly bound hydrocarbon species is reached almost twice as fast as in the case of the bare Fe_3O_4 film. A number of reasons may account for this fact. First, the adsorption properties of the support might be modified as a result of Pd deposition and stabilization under oxidizing conditions in such a way that considerably less butene can be adsorbed on the support itself as compared to the pristine oxide film. However, this effect alone cannot solely account for the length of the induction period on the supported catalyst. In fact, the length of the induction period decreases further with increasing temperature (see Figure 7). This suggests that the build-up of the threshold coverage of hydrocarbon species during the induction period may involve thermally activated steps taking place on the Pd particles such as partial dehydrogenation of the butene. Apparently, such partly dehydrogenated hydrocarbon species may be easier formed at elevated temperatures, and hence rapidly saturate the surface. It should be pointed out, however, that the hydrocarbon uptake observed in this induction period may also include some adsorption of molecular butene, in particular at the later stages of the dose, after the formation of partly dehydrogenated hydrocarbon residues. The relative fractions of carbonaceous deposits versus molecularly adsorbed olefin resulting from the uptake during the induction period are determined by the relative magnitudes of the rates of dehydrogenation versus adsorption−desorption equilibrium of molecular butene at a given temperature. Therefore the length of the induction period and the relative abundance of the different hydrocarbon species formed on the surface are expected to depend in complex way on the reaction temperature, a way not easy to unravel from our experimental data.

Also, in contrast to what was observed on the pristine oxide surface, significant conversion of the *cis*-2-butene is seen on the Pd/Fe_3O_4 catalyst after the initial adsorption of the butene described above. The formation rates of *trans*-2-butene-d_1, *cis*-

2-butene-d_2, and butane-d_2 and -d_3 at 200 K all exhibit an induction period of about 40 s (corresponding to 20 s of total exposure time in the 5 initial pulses), coinciding with the duration of the strong adsorption regime seen for the reactant (Figure 6). This fact indicates that the initial strong adsorption mode on the supported system involves the buildup of a threshold coverage of butene and/or other hydrocarbon species on the Pd particles that do not directly participate in but prepare the surface for the subsequent reactions. Only after the metal surface is saturated with those spectator hydrocarbon species the butene catalytic conversion becomes possible.

Once the conversion starts, the rates of all the reaction pathways listed above show a distinct transient behavior, with comparable rates that reach maxima at about 80 s and decrease to zero after about 300−400 s for H-D exchange/isomerization and after 200 s for deuteration.

Figure 7 displays the reaction rates of *trans*-2-butene-d_1 production for a series of temperatures between 190 and 260 K. Here, it should be emphasized that the reported experiments were carried out at temperatures well above those required for the desorption of the olefins. Therefore, they reflect the kinetics of the chemical reactions on the surface, not that of the desorption of the hydrocarbons. Similar kinetics are observed for the production of *trans*-2-butene-d_1 between 190 and 210 K, with the transient behavior comprising an induction period, an initial high activity, and an asymptotic decay in reaction rate to zero after a few hundreds of seconds. However, the reactivity pattern markedly changes when the reaction is carried out at 250 and 260 K. First, the surface follows a considerably shorter induction period than in the low-temperature range, of only 8 s at 250 K (compared to 20 s at 200 K). In addition, there is a persistent catalytic activity toward H-D exchange/isomerization at 250−260 K even after prolonged periods of time. In fact, the activity at these temperatures was probed for much longer time scales than that displayed in Figure 7, and several turnovers were obtained (over a period of more than 2 h) without any significant reduction in the steady-state reaction rates of cis−trans isomerization. This is perhaps the most important observation from this experiment, because, to the best of our knowledge, sustained catalytic activity has not been achieved under vacuum before, not even in molecular beam experiments with large excesses of hydrogen in the gas mixture.[92,93]

The substantial decrease in the induction period seen at 250−260 K suggests the formation of a specific type of strongly adsorbed hydrocarbon species on the Pd particles at these temperatures, which involves a thermally activated step. It is important to note that this transition roughly coincide with the onset of hydrogen desorption seen in TPD, which is associated with the first step of *cis*-2-butene decomposition on the Pd surface. Even though it is not clear from the TPD data if the hydrogen released at 250 K is kinetically limited by alkene dissociation or by recombinative hydrogen desorption, the abrupt change in the length of the induction period in the MB runs strongly suggests that butene decomposition takes place in this temperature range. Based on information from the literature, it can be speculated that the first dissociation step presumably involves abstraction of the inner hydrogen atoms in the adsorbed 2-butene and leads to the formation of di-σ bonded 2-butyne species.[103]

As the possible reasons for the transition from limited conversion to the persistent catalytic activity seen around 250 K in Figure 7 are discussed, it is worth remembering that the lack of sustained conversion in vacuum experiments is usually ascribed to the strong inhibition of dissociative hydrogen/deuterium adsorption on the metal surfaces induced by the presence of strongly bonded hydrocarbon species.[2,44] Consistent with this is the fact that both hydrogenation and isomerization rates for *cis*-2-butene on Pt(111) follow a near-first-order dependence on the hydrogen pressure and a zero dependence on the hydrocarbon pressure.[118] On the basis of these considerations, it appears that in the low-temperature region the reactions observed in the initial stages of the MB runs involve only the hydrogen (or deuterium) adsorbed at the very beginning of those runs, before the surface is exposed to the butene beam. Once the hydrocarbon exposure starts, however, the butene appears to form strongly adsorbed hydrocarbon surface species (most likely a di-σ species) without any deuterium consumption, until a threshold coverage of those species is reached. After this induction period, additional butene may react with the deuterium already present on the surface, hence the high initial reaction rates for both H-D exchange/isomerization and hydrogenation reaction pathways seen in Figure 7. However, further dissociative adsorption of deuterium is prevented by the hydrocarbon deposits formed during early butene decomposition, so the activity of the surface vanishes after the initially available deuterium is consumed.

Following the same reasoning, it can be said that the sustained catalytic activity toward isomerization/H-D exchange observed above 250 K attests to the ability of the Pd particles to dissociatively adsorb deuterium at these temperatures, in competition with butene adsorption and in the presence of partly dissociated hydrocarbon species on the surface. This was in fact proven directly in isotope switching experiments, where the hydrogenation and H-D exchange reactions could be reversibly turned on and off by either interchanging H_2 and D_2 beams or switching either one off and back on (data not shown). Two possible reasons might account for this phenomenon. First, the more strongly dehydrogenated hydrocarbon spectator species that form on the surface above 250 K might have a smaller footprint, and may leave some open metal sites available for deuterium dissociative adsorption. Second, faster butene desorption (as compared to the low temperature case) may result in a lower steady-state coverage of the reversibly adsorbed butene, diminishing the potential poisoning effect of those hydrocarbon species toward the dissociative adsorption of deuterium. Both tendencies result in the reduced poisoning of the surface by hydrocarbons, and to the sustained ability of Pd particles to dissociatively adsorbed deuterium under reaction conditions. These results demonstrate for the first time, to the best of our knowledge, that alkene conversion can be maintained over long times under the vacuum conditions[92,93] and argue strongly for the power of using realistic models such as ours to simulate real catalysis; it appears that similar hydrogen uptake is not possible on single-crystal surfaces covered with carbonaceous deposits.[79] It is worth noting, though, that the reaction probabilities measured under our conditions are on the order of a few percent. For comparison, a typical alkene catalytic hydrogenation process carried out around room temperature and under atmospheric pressures exhibits reaction probabilities on the order of $10^{-5}-10^{-10}$.[2,5,105] At present we do not have a fully satisfactory explanation for the unique high activity of our model catalyst.

3.5. Selectivity between Isomerization and Hydrogenation on Pd/Fe_3O_4. The TPD data discussed in section 3.3 indicate that not only activity but also selectivity toward different reaction pathways might be affected by the presence of different carbonaceous species on the surface. To study this dependency in more detail, comparative pulsed isothermal MB experiments

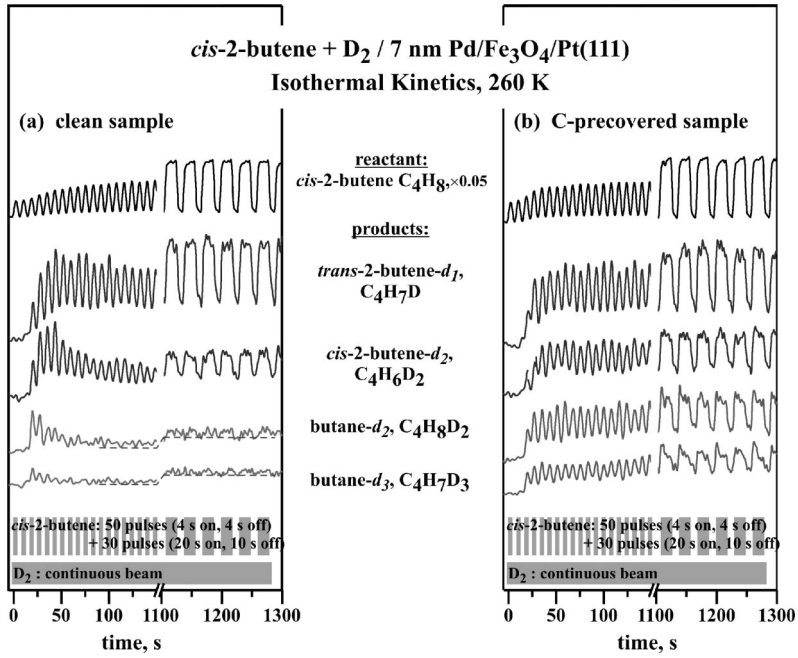

Figure 8. Results from isothermal pulsed molecular beam (MB) experiments on the conversion of *cis*-2-butene with D_2 at 260 K on initially clean (a) and C-precovered (b) Pd/Fe_3O_4 model catalysts. The latter sample was prepared by performing one TPD cycle as shown in Figure 4 prior to the MB run. Data are reported here for the evolution of the reaction rates as a function of time for the reactant (*cis*-2-butene) and for the main four products (*trans*-2-butene-d_1, *cis*-2-butene-d_2, butane-d_2, and butane-d_3). They indicate that while on the initially clean surface only sustained isomerization is possible (left panel), both isomerization and hydrogenation production persist on the surface precovered with carbon deposits (right panel).

were performed at 260 K on both initially clean and carbon-precovered Pd particles. The Pd particles precovered with carbon were prepared following the procedure used in the TPD experiments, namely, by dosing 280 L of D_2 and 0.85 L of the alkene sequentially at 100 K and then annealing to approximately 500 K. As discussed earlier, this treatment produces highly dehydrogenated carbonaceous species containing only a few if any hydrogen atoms. For the sake of simplicity, we will refer to these species as carbon in the following discussion.

Figure 8 shows the time evolution of the signals for the original *cis*-2-butene and for the four main reaction products (*trans*-2-butene-d_1, *cis*-2-butene-d_2, butane-d_2, and butane-d_3) as a function of reaction time in experiments carried out at 260 K starting with the clean (left) and carbon-covered (right) surfaces. As discussed in the previous section, on the initially clean surface, a transient behavior is seen for all products, consisting of an induction period in which no reaction products are detected (and only the uptake of the *cis*-2-butene is observed) followed by a period of high activity for both isomerization/H-D exchange and deuteration. However, whereas the isomerization rates to *trans*-2-butene-d_1 and *cis*-2-butene-d_2 are sustained over longer periods of time at this temperature, the deuteration rates to butane-d_2 and butane-d_3 return to zero.

Interestingly, the surface precovered with carbon follows an induction period for the uptake of butene similar to that seen with the clean surface. This indicates that carbon contamination does not significantly change the total surface area accessible for butene adsorption, an observation corroborated by the CO-titration IR spectra obtained on both clean and carbon-precovered Pd particles (see Figure 5): carbon contamination was found to affect mostly the defect sites (edges and corners of the Pd particles) without reducing adsorption capacity of the (111) facets, which represent the majority of the surface sites. In addition, recent theoretical calculations on Pd clusters show that the binding energy of carbon on edges is about the same as in the subsurface region near those edges.[116] It is therefore even possible that the carbon in the 500 K-pretreated surfaces diffuses to the inside of the particle through its edges.

Also surprising here is the observation that not only isomerization but also hydrogenation to both butane-d_2 and butane-d_3 can be sustained under steady-state conditions on the carbon-covered surface. Additionally, the two competing reaction pathways were found to exhibit very different transient behavior. Figure 9 shows the time evolution of the reaction rates for isomerization and hydrogenation, together with the time evolution of the *cis*-2-butene in the chamber, during the individual *cis*-2-butene long pulses on the initially clean (left) and carbon-precovered (right) surfaces (averaged over the last 30 pulses). The transient kinetic data show that both isomerization rates simply follow the time evolution of the reactant, suggesting that they are limited by the rate of *cis*-2-butene adsorption under the given conditions. In contrast, both hydrogenation rates on the C-precovered surface are high at the beginning of the *cis*-2-butene exposure but decrease considerably over the duration of the pulse. This behavior can be explained by noting that the surface is saturated with deuterium atoms before the start of the alkene exposure (because the deuterium beam is kept on continuously) and hence is highly reactive toward deuteration as soon as the alkene becomes available at the beginning of the butene pulse. However, as the reaction proceeds, that deuterium is consumed, and the initially high surface coverage of deuterium decreases to a new lower steady-state level because of the partial poisoning of the surface by butene.

An additional consideration here is the fact that, according to the Horiuti−Polanyi mechanism, both H-D exchange/isomerization and hydrogenation (deuteration) reactions involve two elementary surface steps, the first of which is the formation of a common surface 2-butyl intermediate.[9,10] The fast isomerization and deuteration seen at the beginning of each pulse suggest that butyl formation is fast, and that the selectivity is

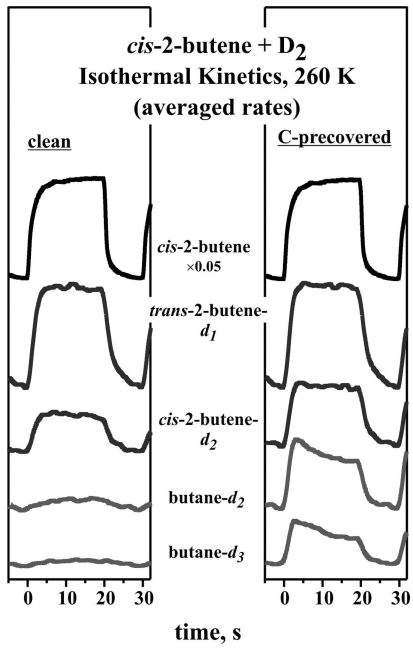

Figure 9. Average reaction rates as a function of time during each cycle in the latter part of the isothermal MB experiments reported in Figure 8. Data are again contrasted for the initially clean (left panel) versus carbon-precovered (right panel) Pd particles. The rates were calculated by averaging the steady-state reaction rates from the last 30 long pulses of the experiment.

defined by competition between the two subsequent reactions, β-hydride elimination for the exchange versus reductive elimination with a coadsorbed deuterium atom for the deuteration. The former step does not require any additional reactants, and therefore follows closely the kinetics of butyl formation, which in turn depends on the uptake of the butene. The latter, on the other hand, requires an additional deuterium surface atom. The observed transient behavior suggests that the hydrogenation rate is controlled by the number of accessible deuterium atoms, that is, by the dissociative adsorption of deuterium.

It is particularly puzzling to see such dramatic change in selectivity with changes in the nature of the carbonaceous deposits present on the surface. Here it should be kept in mind that even when starting with a clean surface, strongly bonded carbonaceous deposits do form and persist after the initial induction period in the MB isothermal experiments. So it is the different nature of those deposits when annealing to ~500 K rather than their mere presence on the surface what leads to the promotion of the hydrogenation reactions. In fact, annealing the predeposited adsorbed butene to only ~350 K is not sufficient to achieve this behavior (data not shown). Based on the TPD data shown in Figure 4, we suggest that the more active surface may contain highly dehydrogenated surface species, perhaps even carbon alone in carbidic form, crucially, that carbon may be present in the subsurface (see below).

The predeposited carbon must be capable of performing at least two functions in order to help preserve the catalytic activity of the surface. On the one hand, it must block extensive alkene dehydrogenation pathways, at least when a set coverage of carbonaceous deposits on the surface is reached, otherwise the surface would eventually be poisoned by those. On the other, it must also leave some exposed metal sites available for deuterium adsorption and alkene conversion. Both are possible if the different reactions require catalytic sites with different Pd ensemble sizes, or if they occur on different surface sites. That way, the carbon can be seen as selectively promoting some reactions at the expense of others, at least in relative terms. Indeed, dehydrogenation steps are believed to require large numbers of metal atoms, so those could be poisoned easily.[2] Hydrogenation, either to alkyl species or to alkanes, may be possible on smaller sites and, therefore, still be feasible on partially carbon-covered surfaces. Even smaller sites may be capable of sustaining the H-D exchange path; hence, the sustained activity seen for that reaction even when starting from the clean surface (where steady-state alkane production is not possible). Certainly, different adsorption requirements are applicable to alkenes compared to those for hydrogen/deuterium, as manifested by the different results that are often obtained in coadsorption TPD experiments depending on the order in which the two reactants are dosed on the surface.[7,14] Moreover, adsorption of different hydrocarbon fragments requires different adsorption geometries, and hydrogenation and dehydrogenation steps also involve different ensembles of surface atoms.[8,10,119] Most of the results reported to date on surface-science studies on model systems involving hydrocarbon chemistry are supportive of the idea of selectivity in hydrogenation versus dehydrogenation steps being dependent on the size and nature of the surface sites available for reaction.

Alternatively, it could be argued that in the case of the pretreatment of the Pd particles at 500 K the nature of the surface changes because of the presence of carbon in the subsurface. As mentioned above, there are at least three reasons to believe that the surface in that case is fairly clean, and that most of the carbon initially deposited by butene adsorption and decomposition diffuses into the subsurface region after annealing to 500 K: (i) the CO RAIRS titration spectra in Figure 5 show that only defect sites are affected by dosing butene on the surface and annealing to 500 K, the majority of the surface sites on the (111) facets appear to remain free; (ii) the induction period for the uptake of the olefin in the MB experiments is the same for both clean and pretreated surfaces (Figure 8); and (iii) the steady-state isomerization rates for the mono H-D exchanged product are similar on the initially clean and C-precovered surfaces. Perhaps the subsurface carbon modifies the electronic nature of the surface palladium atoms, and that affects the behavior of the catalyst toward alkene hydrogenation and/or dehydrogenation (but apparently not toward H-D exchange or double bond isomerization) reactions. It should be mentioned that Pd surfaces pretreated by adsorbing butene at low temperature and annealing to 350 instead of 500 K do not facilitate the catalytic hydrogenation of the olefin, and behave quite similarly to the case of starting with the clean surface. Clearly, in that case the carbonaceous deposits formed by the pretreatment are quite similar to those that form during the induction period of the MB experiments and do not modify the performance of the surface in the way that the "carbidic" subsurface species do.

A third possibility to account for the changes in selectivity reported here with surface pretreatment is that the hydrogenation catalytic activity induced by strongly bound carbonaceous species on Pd particles is due to a change of the hydrogen adsorption state in the presence of the deposited carbon. Previously, the origin of the hydrogenation activity observed on dispersed Pd particles but not on single crystals has been ascribed to the unique ability of the small metal clusters to bind hydrogen in a special weakly bound state.[37] Recent NRA (nuclear reaction analysis) experiments on the hydrogen distribution in the dispersed Pd particles supported on an oxide film provided clear experimental proof for those weakly bound hydrogen atoms being a subsurface/bulk species.[120] Our experimental data support this idea that two different forms of

hydrogen (deuterium) may be involved in the competing isomerization and hydrogenation reaction pathways. This is illustrated by the results in Figure 8 in particular those for the reaction rates at 260 K for isomerization to *trans*-2-butene-d_1 and deuteration to butane-d_2 on the initially clean particles. The data show that when the reaction starts, after the clean particles have been saturated with deuterium at the beginning of the experiment, both reaction pathways display about the same reaction rates. However, the hydrogenation rate drops soon afterward, and reaches a value of zero under steady-state conditions. The isomerization rate, on the other hand, remains as high as at the beginning of the experiment. The two reactions share a common hydrocarbon reaction intermediate, a butyl surface species produced by the half-hydrogenation of the adsorbed olefin (see the reaction scheme in Figure 1), which is formed readily on the surface as indicated by the sustainability of the H-D exchange reaction. Therefore all differences in the reaction kinetics of the H-D exchange/isomerization and hydrogenation pathways are most likely related to their different requirements in deuterium atoms. The observed selective suppression of only the hydrogenation pathway on the initially clean surface under steady-state conditions is not likely to be explained simply by changes in hydrogen (deuterium) surface coverages since both reactions require deuterium additions and exhibit similar reaction orders on deuterium (hydrogen) pressures.[118] More likely, the vanishing hydrogenation activity can be rationalized by assuming that a special type of deuterium atoms is required for the second hydrogenation step (conversion of butyl to butane). That special deuterium species may form during the initial deuterium uptake, but become depleted during the course of the reaction. In line with the previous observations we assume that this special type of deuterium atoms might be a weakly bound subsurface/bulk species. It could be argued that deposition of strongly bound carbonaceous species weakens the metal-deuterium bond and makes it possible to replenish the population of such special deuterium under steady-state conditions, resulting in the sustained hydrogenation conversion.

Indeed, TPD measurements carried out on the clean and carbon precovered Pd particles show that the distribution of hydrogen atoms is strongly shifted toward lower temperatures on surfaces precovered with carbon, suggesting that such weakly bonded species may be the ones responsible for the production of the alkane.[36] Currently, the experiments are under way, where the distribution of the hydrogen species under isothermal reaction conditions is investigated by means of NRA both on the clean and carbon-precovered Pd particles, which will be a subject of a publication in the near future.[121]

Finally, it should be pointed out that the proposed explanations of the observed unique catalytic behavior seen here with the supported palladium model system are speculative, and should be considered rather as working hypotheses to be tested in further experiments.

4. Conclusions

The catalytic conversion of *cis*-2-butene on a well-defined model supported catalyst was investigated under UHV conditions by using a combination of RAIRS, TPD, and molecular beam experiments. Emphasis was placed on exploring the role of the carbonaceous deposits typically present under catalytic reaction conditions on the activity and selectivity toward different reaction pathways, in particular cis−trans isomerization versus hydrogenation.

The Pd model catalysts used consisted of Pd particles of 7 nm average size with predominant (111) facets (but also exposing a small fraction of (100) surfaces) deposited on a well-ordered Fe_3O_4 film grown on Pt(111) as a support. The following key conclusions were reached:

1. *cis*-2-butene adsorbs molecularly on the pristine Fe_3O_4 film either clean or after predosing deuterium. Two adsorption modes were identified in molecular beam experiments, a strong and irreversible state that populates first, at the start of the olefin uptake, and a second, weaker and reversible adsorption regime that develops afterward. No catalytic activity toward the conversion of *cis*-2-butene with deuterium was observed on the Fe_3O_4 support.

2. Starting with a Pd/Fe_3O_4 catalyst predosed with deuterium, thermal activation of adsorbed *cis*-2-butene in TPD experiments leads to several reaction pathways, including dehydrogenation, cis−trans isomerization (which is accompanied by H-D exchange), and hydrogenation. Dehydrogenation of the alkene was also found to proceed, in several consecutive steps. Carbon deposition on the Pd particles by annealing of the surface covered with the olefin at 500 K leads to inhibition of the dehydrogenation reaction pathways, and increases molecular desorption of the reactant.

3. The isothermal uptake of *cis*-2-butene on Pd/Fe_3O_4 goes through an induction period followed by a period of high reactivity toward both cis−trans isomerization and hydrogenation. The induction period is associated with accumulation of strongly adsorbed hydrocarbon species, which might include molecularly adsorbed butene and/or partly dehydrogenated butene derivatives depending on the reaction temperature.

4. At low (190−210 K) temperatures, the initial reactivity transient described above is followed by a decrease in all reaction rates until returning to zero after a few hundreds of seconds. This behavior is likely to be the consequence of the strong inhibition of the dissociative deuterium chemisorption by the presence build-up of bulky hydrocarbon species, most likely di-σ bonded butene.

5. At temperatures above 250 K, sustained catalytic activity toward cis−trans isomerization is possible. This is, to the best of our knowledge, the first time that such sustained catalytic behavior has been seen under vacuum conditions. The onset of the steady-state reactivity is accompanied by the reduction of the induction period in the initial olefin uptake. This behavior suggests that (i) the initial accumulation of the strongly bound hydrocarbon species that form on the surface during the induction period above 250 K is a thermally activated process, which produces partly dehydrogenated carbonaceous deposits, probably exhibiting a smaller surface area footprint, and (ii) the catalyst surface is still able to dissociatively adsorb deuterium above 250 K, even in competition with the molecular butene adsorption and in the presence of surface butene derivatives. However, despite of the observed sustained catalytic activity toward cis−trans isomerization, the hydrogenation reaction pathway cannot be maintained on the initially clean surface.

6. On surfaces pretreated by adsorbing *cis*-2-butene at 100 K and annealing at 500 K, a different catalytic behavior is seen where both reaction pathways, cis−trans isomerization and hydrogenation, are sustained over long periods of time. Clearly, carbon deposition aids in the sustainability of the hydrogenation reaction pathways, and thus critically controls activity and selectivity. Several pieces of evidence point to the wide availability of surface sites, in particular in the (111) facets, and to the presence of subsurface carbon in this case.

A discussion of the possible reasons for the observed phenomena was provided. The facilitation of the catalytic hydrogenation reaction pathway in particular could be possibly

ascribed to a combination of the following factors: (i) different space requirements for the H-D exchange/isomerization and hydrogenation competing reaction pathways, (ii) an electronic modification of the surface by the presence of subsurface carbon, and/or (iii) changes in the distribution of deuterium between weakly and strongly bound adsorption states, which may exhibit different reactivity toward hydrogenation.

Acknowledgment. Financial support by the following agencies is gratefully acknowledged: Deutsche Forschungsgemeinschaft, Fonds der Chemischen Industrie, and the U.S. National Science Foundation. F.Z. thanks the Alexander-von-Humbold Foundation for a senior scientist award. Finally, we thank Prof. R.J. Madix for helpful discussions.

References and Notes

(1) Ponec, V.; Bond, G. C. *Catalysis by Metals and Alloys*; Elsevier: Amsterdam, 1995.

(2) Bond, G. C. *Metal-Catalysed Reactions of Hydrocarbons*; Springer Science: New York, 2005.

(3) Taylor, T. I. In *Catalysis*; Emmett, P. H., Ed.; Reinhold: New York, 1957: Vol. 5, pp 257−403.

(4) Kemball, C. In *Advances in Catalysis and Related Subjects*; Eley, D. D., Selwood, P. W., Weisz, P. B., Eds.; Academic Press: New York, 1959; Vol. 11, pp 223−262.

(5) Horiuti, J.; Miyahara, K. Hydrogenation of Ethylene on Metallic Catalysts. *Report NSRDS-NBC No. 13*; National Bureau of Standards: Gaithersberg, MD, 1968.

(6) Somorjai, G. A. *Introduction to Surface Science Chemistry and Catalysis*; John Wiley & Sons: New York, 1994.

(7) Zaera, F. *Prog. Surf. Sci.* **2001**, *69*, 1.

(8) Ma, Z.; Zaera, F. *Surf. Sci. Rep.* **2006**, *61*, 229.

(9) Horiuti, J.; Polanyi, M. *Trans. Faraday. Soc.* **1934**, *30*, 1164.

(10) Zaera, F. *Chem. Rev.* **1995**, *95*, 2651.

(11) Zaera, F. *Acc. Chem. Res.* **1992**, *25*, 260.

(12) Koestner, R. J.; Frost, J. C.; Stair, P. C.; Van Hove, M. A.; Somorjai, G. A. *Surf. Sci.* **1982**, *116*, 85.

(13) Zaera, F. *Langmuir* **1996**, *12*, 88.

(14) Zaera, F. *J. Catal.* **1990**, *121*, 318.

(15) Neimantsverdriet, J. W.; Borg, H. G.; van Hardeveld, R. M.; van Saten, R. A. *Recueil Travaux Chim. Pays-Bas* **1996**, *115*, 486.

(16) Guo, X.-C.; Madix, R. J. *J. Catal.* **1995**, *155*, 336.

(17) Vasquez, N., Jr.; Madix, R. J. *J. Catal.* **1998**, *178*, 234.

(18) Zaera, F. *J. Phys. Chem.* **1990**, *94*, 5090.

(19) Janssens, T. V. W.; Zaera, F. *Surf. Sci.* **1995**, *344*, 77.

(20) Janssens, T. V. W.; Stone, D.; Hemminger, J. C.; Zaera, F. *J. Catal.* **1998**, *177*, 284.

(21) Zaera, F.; Chrysostomou, D. *Surf. Sci.* **2000**, *457*, 89.

(22) Lee, I.; Zaera, F. *J. Phys. Chem. B* **2005**, *109*, 2745.

(23) Lee, I.; Zaera, F. *J. Phys. Chem. C* **2007**, *111*, 10062.

(24) Salmerón, M.; Somorjai, G. A. *J. Phys. Chem.* **1982**, *86*, 341.

(25) Lee, I.; Zaera, F. *J. Am. Chem. Soc.* **2005**, *127*, 12174.

(26) Morales, R.; Zaera, F. *J. Phys. Chem. B* **2006**, *110*, 9650.

(27) Morales, R.; Zaera, F. *J. Phys. Chem. C*. in press.

(28) Hwu, H. H.; Eng, J.; Chen, J. G. *J. Am. Chem. Soc.* **2002**, *124*, 702.

(29) Khan, N. A.; Chen, J. G. *J. Vac. Sci. Technol. A* **2003**, *21*, 1302.

(30) Murillo, L. E.; Khan, N. A.; Chen, J. G. *Surf. Sci.* **2005**, *594*, 27.

(31) Burke, M. L.; Madix, R. J. *J. Am. Chem. Soc.* **1991**, *113*, 3675.

(32) Burke, M. L.; Madix, R. J. *Surf. Sci.* **1990**, *237*, 20.

(33) Zaera, F. *J. Phys. Chem.* **1990**, *94*, 8350.

(34) Zaera, F. *Catal. Lett.* **2003**, *91*, 1.

(35) Shaikhutdinov, Sh.; Heemeier, M.; Bäumer, M.; Lear, T.; Lennon, D.; Oldman, R. J.; Jacson, S. D.; Freund, H.-J. *J. Catal.* **2001**, *200*, 330.

(36) Shaikhutdinov, Sh.K.; Frank, M.; Bäumer, M.; Jackson, S. D.; Oldman, R. J.; Hemminger, J. C.; Freund, H.-J. *Catal. Lett.* **2002**, *80*, 115.

(37) Doyle, A. M.; Shaikhutdinov, Sh.K.; Jackson, S. D.; Freund, H.-J. *Angew. Chem., Int. Ed.* **2003**, *42*, 5240.

(38) Doyle, A. M.; Shaikhutdinov, Sh.K.; Freund, H.-J. *J. Catal.* **2004**, *223*, 444.

(39) Doyle, A. M.; Shaikhutdinov, Sh.K.; Freund, H.-J. *Angew. Chem., Int. Ed.* **2005**, *44*, 629.

(40) Thomson, S. J.; Webb, G.; Chem, J. *Chem. Commun.* **1976**, *526*.

(41) Davis, S. M.; Zaera, F.; Somorjai, G. A. *J. Catal.* **1982**, *77*, 439.

(42) Zaera, F. *Chem. Rec.* **2005**, *5*, 133.

(43) Twigg, G. H. *Disc. Faraday Soc.* **1950**, *8*, 152.

(44) Zaera, F.; Somorjai, G. A. In *Hydrogen Effects in Catalysis: Fundamentals and Practical Applications*; Paál, Z., Menon, P. G., Eds.; Marcel Dekker: New York, 1988; pp 425−447.

(45) Campbell, C. T. *Adv. Catal.* **1989**, *36*, 1.

(46) Arafa, E. A.; Webb, G. *Catal. Today* **1993**, *17*, 411.

(47) Houzvicka, J.; Pestman, R.; Ponec, V. *Catal. Lett.* **1995**, *30*, 289.

(48) Cremer, P.; Stanners, C.; Niemantsverdriet, J. W.; Shen, Y. R.; Somorjai, G. *Surf. Sci.* **1995**, *328*, 111.

(49) Janssens, T. V. W.; Zaera, F. *J. Phys. Chem.* **1996**, *100*, 14118.

(50) Zaera, F.; French, C. R. *J. Am. Chem. Soc.* **1999**, *121*, 2236.

(51) Kesmodel, L. L.; Gates, J. A. *Surf. Sci.* **1981**, *111*, L747.

(52) Beebe, T. P., Jr.; Yates, J. T., Jr. *J. Am. Chem. Soc.* **1986**, *108*, 663.

(53) Kesmodel, L. L.; Dubois, L. H.; Somorjai, G. A. *Chem. Phys. Lett.* **1978**, *56*, 267.

(54) Skinner, P.; Howard, M. W.; Oxton, I. A.; Kettle, S. F. A.; Powell, D. B.; Sheppard, N.; Chem, J. *Faraday Trans. II* **1981**, *77*, 1203.

(55) Davis, S. M.; Zaera, F.; Gordon, B.; Somorjai, G. A. *J. Catal.* **1985**, *92*, 240.

(56) Zaera, F. *J. Am. Chem. Soc.* **1989**, *111*, 4240.

(57) Ohtani, T.; Kubota, J.; Kondo, J. N.; Hirose, C.; Domen, K. *J. Phys. Chem. B* **1999**, *103*, 4562.

(58) Ko, M. K.; Frei, H. *J. Phys. Chem. B* **2004**, *108*, 1805.

(59) Koel, B. E.; Bent, B. E.; Somorjai, G. A. *Surf. Sci.* **1984**, *146*, 211.

(60) Nieskens, D. L. S.; van Bavel, A. P.; Curulla Ferre, D.; Niemantsverdriet, J. W. *J. Phys. Chem. B* **2004**, *108*, 14541.

(61) Greenlief, C. M.; Radloff, P. L.; Zhou, X. L.; White, J. M. *Surf. Sci.* **1987**, *191*, 93.

(62) Marinova, T. S.; Kostov, K. L. *Surf. Sci.* **1987**, *181*, 573.

(63) Zaera, F.; Hall, R. B. *Surf. Sci.* **1987**, *180*, 1.

(64) Stuve, E. M.; Madix, R. J.; Brundle, C. R. *Surf. Sci.* **1985**, *152/153*, 532.

(65) Liu, Z.-M.; Zhou, X.-L.; Buchanan, D. A.; Kiss, J.; White, J. M. *J. Am. Chem. Soc.* **1992**, *114*, 2031.

(66) Zaera, F.; Bernstein, N. *J. Am. Chem. Soc.* **1994**, *116*, 4881.

(67) Hatzikos, G. H.; Masel, R. I. *Surf. Sci.* **1987**, *185*, 479.

(68) Ormerod, R. M.; Lambert, R. M.; Hoffmann, H.; Zaera, F.; Wang, L. P.; Bennett, D. W.; Tysoe, W. T. *J. Phys. Chem.* **1994**, *98*, 2134.

(69) Demuth, J. E. *Surf. Sci.* **1978**, *76*, L603.

(70) Stroscio, J. A.; Bare, S. R.; Ho, W. *Surf. Sci.* **1984**, *148*, 499.

(71) Zaera, F.; Hall, R. B. *J. Phys. Chem.* **1987**, *91*, 4318.

(72) Backman, A. L.; Masel, R. I. *J. Phys. Chem.* **1990**, *94*, 5300.

(73) Nishijima, M.; Yoshinobu, J.; Sekitani, M.; Onchi, M. *J. Chem. Phys.* **1989**, *90*, 5114.

(74) Koestner, R. J.; Frost, J. C.; Stair, P. C.; van Hove, M. A.; Somorjai, G. A. *Surf. Sci.* **1982**, *116*, 85.

(75) Avery, N. R.; Sheppard, N. *Surf. Sci. Lett.* **1986**, *169*, L367.

(76) Chesters, M. A.; De La Cruz, C.; Gardner, P.; McCash, E. M.; Pudney, P.; Shahid, G.; Sheppard, N. *J. Chem. Soc., Faraday Trans.* **1990**, *86*, 2757.

(77) Cremer, P. S.; Su, X.; Shen, Y. R.; Somorjai, G. A. *J. Phys. Chem.* **1996**, *100*, 16302.

(78) Bent, B. E.; Mate, C. M.; Crowell, J. E.; Koel, B. E.; Somorjai, G. A. *J. Phys. Chem.* **1987**, *91*, 1493.

(79) Zaera, F.; Chrysostomou, D. *Surf. Sci.* **2000**, *457*, 71.

(80) Pettiette-Hall, C. L.; Land, D. P.; McIver, R. T., Jr.; Hemminger, J. C. *J. Am. Chem. Soc.* **1991**, *113*, 2755.

(81) Henn, F. C.; Diaz, A. L.; Bussell, M. E.; Hugenschmidt, M. B.; Domagala, M. E.; Campbell, C. T. *J. Phys. Chem.* **1992**, *96*, 5965.

(82) Xu, C.; Koel, B. E.; Newton, M. A.; Frei, N. A.; Campbell, C. T. *J. Phys. Chem.* **1995**, *99*, 16670.

(83) Scoggins, T. B.; White, J. M. *J. Phys. Chem. B* **1997**, *101*, 7958.

(84) Bratlie, K. M.; Flores, L. D.; Somorjai, G. A. *Surf. Sci.* **2005**, *599*, 93.

(85) Zhdanov, V. P.; Kasemo, B. *Surf. Sci. Rep.* **2000**, *39*, 25.

(86) Henry, C. R. *Surf. Sci. Rep.* **1998**, *31*, 231.

(87) Bäumer, M.; Freund, H.-J. *Prog. Surf. Sci.* **1999**, *61*, 127.

(88) Campbell, C. T.; Grant, A. W.; Starr, D. E.; Parker, S. C.; Bondzie, V. A. *Top. Catal.* **2001**, *14*, 43.

(89) St, T. P.; Goodman, D. W. *Top. Catal.* **2000**, *13*, 5.

(90) Schalow, T.; Brandt, B.; Laurin, M.; Starr, D.; K., Sh.; Shaikhutdivov; Libuda, J.; Freund, H.-J. *Catal. Lett.* **2006**, *107*, 189.

(91) Libuda, J.; Meusel, I.; Hartmann, J.; Freund, H.-J. *Rev. Sci. Instrum.* **2000**, *71*, 4395.

(92) Öfner, H.; Zaera, F. *J. Phys. Chem.* **1997**, *101*, 396.

(93) Brown, W. A.; Kose, R.; King, D. A. *Chem. Rev.* **1998**, *98*, 797.

(94) Weiss, W.; Ranke, W. *Prog. Surf. Sci.* **2002**, *70*, 1.

(95) Lemire, C.; Meyer, R.; Henrich, V.; Shaikhutdinov, S. K.; Freund, H.-J. *Surf. Sci.* **2004**, *572*, 103.

(96) Schalow, T.; Brandt, B.; Laurin, M.; Schauermann, S.; Libuda, J.; Freund, H.-J. *J. Catal.* **2006**, *242*, 58.

(97) Kuhrs, C.; Arita, Y.; Weiss, W.; Ranke, W.; Schlögl, R. *Top. Catal.* **2001**, *14*, 111.

(98) Zscherpel, D.; Ranke, W.; Weiss, W.; Schlögl, R. *J. Chem. Phys.* **1998**, *108*, 9506.

(99) Joseph, Y.; Wühn, M.; Niklewski, A.; Ranke, W.; Weiss, W.; Wöll, Ch.; Schlögl, R. *Phys. Chem. Chem. Phys.* **2000**, *2*, 5314.

(100) Manzanares, I. C.; Blunt, V. M.; Peng, J. *J. Phys. Chem.* **1993**, *97*, 3994.

(101) McKean, D. C.; Mackenzie, M. W.; Morrisson, A. R.; Lavalley, J. C.; Janin, A.; Fawcett, V.; Edwards, H. G. M. *Spectrochim. Acta, Part A* **1985**, *41A*, 435.

(102) Barns, A. J.; Howells, J. D. R. *J. Chem. Soc., Faraday Trans. 2* **1973**, *69*, 532.

(103) Avery, N. R.; Sheppard, N. *Proc. R. Soc. London A* **1986**, *405*, 27.

(104) Stuve, E. M.; Madix, R. J. *J. Phys. Chem.* **1985**, *89*, 3183.

(105) de la Cruz, C.; Sheppard, N. *Adv. Catal.* **1996**, *41*, 1.

(106) Hoffmann, F. M. *Surf. Sci. Rep.* **1983**, *3*, 107.

(107) Zaera, F. In *Encyclopedia of Chemical Physics and Physical Chemistry*; Moore, J. H., Spencer, N. D., Eds.; IOP Publishing Inc.: Philadelphia, 2001; Vol. 2, pp 1563−1581.

(108) Bertolini, J. C.; Cassuto, A.; Jugnet, Y.; Massardier, J.; Tardy, B.; Tourillon, G. *Surf. Sci.* **1996**, *349*, 88.

(109) Tourillon, G.; Cassuto, A.; Jugnet, Y.; Massardier, J.; Bertolini, J. C. *J. Chem. Soc., Faraday Trans.* **1996**, *92*, 4835.

(110) Chesters, M. A.; Horn, A. B.; Ilharco, L. M.; Ransley, A. I.; Sakakini, B. H.; Veckerman, J. C. *Surf. Sci.* **1991**, *251/252*, 291.

(111) Wolter, K.; Seiferth, O.; Kuhlenbeck, H.; Bäumer, M.; Freund, H.-J. *Surf. Sci.* **1998**, *399*, 190.

(112) Frank, M.; Bäumer, M. *Phys. Chem. Chem. Phys.* **2000**, *2*, 4265.

(113) Hollins, P. *Surf. Sci. Rep.* **1992**, *16*, 51.

(114) Schauermann, S.; Hoffmann, J.; Johánek, V.; Hartmann, J.; Libuda, J.; Freund, H.-J. *Angew. Chem., Int. Ed.* **2002**, *41*, 2532.

(115) Schauermann, S.; Hoffmann, J.; Johánek, V.; Hartmann, J.; Libuda, J.; Freund, H.-J. *Catal. Lett.* **2002**, *84*, 209.

(116) Yudanov, I. V.; Neyman, K. M.; Rösch, N. *Phys. Chem. Chem. Phys.* **2006**, *8*, 2396.

(117) Stacchiola, D.; Calaza, F.; Zheng, T.; Tysoe, W. T. *J. Mol. Catal. A* **2005**, *228*, 35.

(118) Ch.Yoon, M. X. Yang, G.A. Somorjai. *J. Catal.* **1998**, *176*, 35.

(119) Bent, B. E. *Chem. Rev.* **1996**, *96*, 1361.

(120) Wilde, M.; Fukutani, K.; Naschitzki, M.; Freund, H.-J. *Phys. Rev. B* **2008**, *77*, 113412.

(121) Wilde, M.; Fukutani, K.; Ludwig, W.; Brandt, B.; Fischer, J.-H.; Schauermann, S.; Freund, H.-J. *Angew. Chem.*, submitted.

JP800205J